Available online at www.sciencedirect.com
ScienceDirect
Journal of the European Ceramic Society 27 (2007) 437–443
www.elsevier.com/locate/jeurceramsoc

# Pressureless sintered self-reinforced Y-α-SiAlON ceramics

C.R. Zhou, Z.B. Yu [1], V.D. Krstic *

*Centre for Manufacturing of Advanced Ceramics and Nanomaterials, Department of Mechanical and Materials Engineering, Queen's University, Nicol Hall, 60 Union Street, Kingston, Ontario, Canada K7L 3N6*

Received 1 March 2006; accepted 8 April 2006
Available online 28 July 2006

**Abstract**

Y-doped α-SiAlONs, where the level of aluminum and oxygen was varied, have been successfully densified by pressureless sintering. The effect of parameters such as starting composition, morphology of grains and sintering temperature on densification and mechanical properties of Y-SiAlON ceramics were study. It was found that Y-α-SiAlONs with different compositions could be pressureless sintered in excess of 98% theoretical density at temperatures ranging from 1750 to 1920 °C. The typical microstructure of the SiAlON investigated consists of elongated α-SiAlON grains uniformly distributed in a matrix of equiaxed grains. Fracture toughness of 6.2 MPa $m^{1/2}$ and hardness of 17.6 GPa were found for $Y_{0.667}Si_{8.5}Al_{3.5}O_{1.5}N_{14.5}$ ($m = 2.0$, $n = 1.5$) sintered at 1850 °C. The results indicate that both crack deflection and crack bridging mechanisms of toughening operate in the materials, with the latter being the dominant one.


*Keywords:* SiAlON; Self-reinforcement; Mechanical properties; Sintering

## 1. Introduction

The sintering of silicon nitride usually requires addition of oxides to form liquid necessary for mass transport and densification. This process normally involves the dissolution of alpha silicon nitride in the liquid and precipitation and/or crystallization of beta silicon nitride or beta SiAlON crystals resulting in a microstructure consisting of elongated grains, known to produce self-reinforcement. Unlike silicon nitride which normally crystallizes in the form of elongated grains, α-SiAlON ceramics normally develops grains in equiaxed form exhibiting high hardness and relatively low farcture toughness. Over the last decade, extensive work has been focused on the design of α/β-SiAlON ceramics, which combine the strength and fracture toughness of β-SiAlON and hardness of α-SiAlON to give a tailored combination of mechanical properties.[1] One approach used to toughen the SiAlON ceramics is to select the composition which will provide the conditions under which crystallization of two-phase α/β-SiAlONs is induced. The α- to β-SiAlONs ratio can be controlled by changing the overall composition.[2]

Another approach in achieving the self-reinforced α-SiAlON is to grow elongated α-SiAlON grains in a dense α-SiAlON matrix. It has been observed that the dense α-SiAlON ceramics containing elongated grains can be prepared by carefully selecting the starting composition and/or starting powders.[3,4] For example, Chen and Rosenflanz[3] demonstrated that the elongated α-SiAlON grains could be achieved in a dense α-SiAlON matrix by using a high percentage of β-$Si_3N_4$ phase in the starting powder. It is worth pointing out that over the last few years most fabrication processes used in achieving growth of elongated α-SiAlON grains in dense α-SiAlON ceramics are mainly through hot-pressing technique,[5] which to some extent restrained the formation of elongated grains during sintering. Recently, pressureless sintering technique has been explored using very fine and highly active powders to produce dense α-SiAlONs and to encourage the formation of elongated α-SiAlON grains.[6] In both of these two mechanisms of toughening, the grain width and grain length play an important role in toughening and strengthening of the resultant ceramics.[7] During the sintering process it has been observed that both dimensions of the grain change and it has been custom to correlate the grain width to the level of toughening of the ceramics.[8] Frequently, the effect of grain length and its aspect ratio were not fully explored and their effect on toughening was not evaluated.

* Corresponding author. Tel.: +1 613 533 2760; fax: +1 613 533 6610.
*E-mail address:* krsticv@post.queensu.ca (V.D. Krstic).
[1] Z.B. Yu is now with Northboro Research & Development Centre, HPM, Saint-Gobain, 9 Goddard Road, Northboro, MA 01532, USA.

0955-2219/$ – see front matter © 2006 Elsevier Ltd. All rights reserved.
doi:10.1016/j.jeurceramsoc.2006.04.185

One objective of this paper is to select the composition and sintering conditions under which the growth of elongated α-SiAlON grain is possible in the system Y-α-SiAlON. The other objective is to study the effect of grain morphology on mechanical properties of pressureless sintered Y-α-SiAlON and to elucidate the role that grain aspect ratio, grain width and their volume fraction have on mechanical properties of the resultant ceramics.

## 2. Experimental

Commercially available, high purity α-$Si_3N_4$ powder (UBE E-10) was used as a raw material. Also, commercially available sub-micrometer size $Al_2O_3$ powder (A-16, Alcoa Chemical), high-purity sub-micrometer size $Y_2O_3$ powder (99.99%, Alpha Aesar) and sub-micrometer 'Grade A' AlN powder (99.9%, H.C. Stark) were used as sintering additives. When calculating the composition of the samples, corrections were made for the residual oxygen content in $Si_3N_4$ and AlN. The powder bathes were mixed by ball-milling in a plastic jar using $Si_3N_4$ balls as the milling media. The ball-to-powder weight ratio was held at 5:1. Isopropanol was used as a liquid vehicle and polyethylene glycol as the binder. Milling time was 12 h. The mixed powders were dried at 80 °C for 4 h in order to get rid of isopropanol. The mixed and dried powders were mechanically pressed in a tool-steel die under a pressure of 50 MPa. The green compact in the form of a cylinder had the following dimensions $\phi$ 15 mm × 8 mm. In order to ensure a uniform density, all green compacts were encapsulated in plastic bags using a vacuum packaging machine (HFE Vacuum Systems, The Netherlands) and isostatically pressed under pressure of 225 MPa for 2 min. Sintering was carried out in a vacuum graphite resistant furnace (Model Vacuum Industries Somerville, Massachusetts, USA). Samples were heated at a rate of 4 °C/min to a temperature of 450 °C, followed by a hold of 5 min. The low heating rate was employed in order to allow the organic binder to burn slowly and prevent the damage of the samples. From 450 °C to a final sintering temperature, the heating rate was held at 10 °C/min. Nitrogen was introduced into the furnace at 1050 °C. The gas pressure was ~0.1 MPa. All samples were held at sintering temperature for 120 min before cooling down. The cooling rate was set at 15–20 °C/min. The major phases present in the samples were identified by X-ray diffraction method using a CN2005 X-ray Diffractometter "MINIFLEX" (Rigaku Corp.), Cu $K_\alpha$ radiation ($\lambda = 1.5418$ Å) and Ni filter. Scanning rate was 2°/min and the angle was varied from 10° to 80°. Room temperature Vickers hardness measurements were made on mounted and polished samples using a pyramidal diamond indentor. The standard procedure was to apply a load ($P$) of 10 kg for 10 s. At least eight indentations were made for each sample. The values for hardness were calculated using the following expression[9]:

$$H_V\,(\mathrm{kg/mm^2}) = \frac{0.47P}{a^2} \quad (1)$$

where $P$ is the applied force (N) and $a$ is half the length of the diagonal indentation produced by the diamond indenter. The indentation fracture toughness was calculated using the following expression[9]:

$$K_{IC}\,(\mathrm{MPa\,m^{1/2}}) = \frac{0.15k\left(\frac{c}{a}\right)^{-3/2}H_V g\sqrt{a}}{\phi} \quad (2)$$

where $K_{IC}$ is the fracture toughness (MPa $m^{1/2}$), $\phi$ a constraint (≈3.0), $H_V$ the Vickers hardness (kg/mm$^2$), $g$ the gravitational acceleration (9.81 m/s$^2$), $c$ the average length of the radial cracks, $a$ the average half diagonal length of the indentation (m) and $k$ is a correction factor (≈3.2 for large $c/a$ value).

For microstructural analysis, the samples were first polished on an automatic polishing machine and then chemically etched in hot molten NaOH to reveal their microstructures. The optimum etching condition was determined to be 325 °C for 150 s. Crack propagation and fracture surfaces of the specimens were observed using scanning electron microscope (JSM-840; JEOL, Japan) at an accelerating voltage of 20 kV. A gold coating was applied on the surface of the etched samples in order to minimize the surface charging under electron beam.

The average length, diameter, aspect ratio and volume fraction of the elongated grains (aspect ratio, $l/d > 5$) for Y-α-SiAlON were obtained from the SEM photographs using UTHSCSA 2.00 Image Tool. For each Y-α-SiAlON sample, at least 600 grains were measured on three micrographs in different areas of the sample using the same magnification (5000×). The detailed measurement method is given in reference.[10] Five single-phase α-SiAlON compositions were chosen for the present study and are listed in Table 1.

Table 1
Composition of Y-α-SiAlON ($Y_xSi_{12-(m+n)}Al_{(m+n)}O_nN_{16-n}$) used in this study

| Sample | Symbol | $m$ | $n$ | $x$ |
|---|---|---|---|---|
| (1.0, 1.5) | Y1015 | 1.0 | 1.5 | 0.33 |
| (1.5, 1.5) | Y1515 | 1.5 | 1.5 | 0.50 |
| (2.0, 1.5) | Y2015 | 2.0 | 1.5 | 0.67 |
| (1.0, 1.75) | Y10175 | 1.0 | 1.75 | 0.33 |
| (1.5, 1.25) | Y15125 | 1.5 | 1.25 | 0.50 |

## 3. Results

The X-ray diffraction pattern of sample designated as Y1515 ($Y_{0.5}Si_{9.0}Al_{3.0}O_{1.5}N_{14.5}$, $m = 1.5$, $n = 1.5$) pressureless sintered at 1800 °C is shown in Fig. 1. As can be seen from Fig. 1, only α-SiAlON phase was identified suggesting the existence of a single-phase system. The X-ray diffraction patterns of other compositions designated as Y1015, Y2015, Y10175 and Y15125 also show the presence of only α-SiAlON phase without detectable amount of the second phase. As shown in Fig. 2, the microstructure of Y1515 consists of elongated α-SiAlON grains uniformly distributed in a matrix of equiaxed α-SiAlON grains. The elongated α-SiAlON grains are well developed and have an irregular cross-section perpendicular to the growth direction. The equiaxed α-SiAlON grains have an average width and length of approximately ~1 μm. The black spots, located between the grains, are also revealed in composition Y1515, which were mainly created by the etching-off of the grain boundary phase.

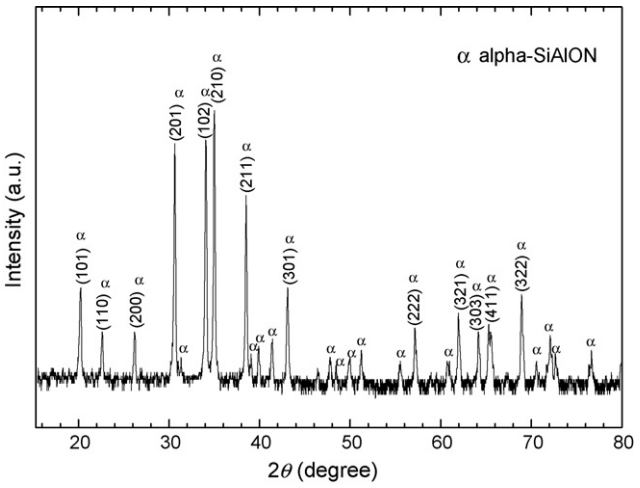


Fig. 1. X-ray diffraction patterns of Y1515 sintered at 1800 °C.

In order to examine the effect of sintering temperature on microstructure and morphology of α-SiAlON grains, the micrographs of a single-phase α-SiAlON (Y2015) sintered at temperatures ranging from 1750 to 1920 °C are give in Fig. 3. At lower temperatures, most of α-SiAlON grains are equiaxed with a small amount of elongated ones. As the sintering temperature increases, the volume fraction and the average size of the elongated grains increase. The volume fraction of elongated grains and their average aspect ratio reach the maximum value at 1850 °C. Above 1850 °C, no appreciable change in average aspect ratio was observed. However, the width of the grain continued to increase. At 1920 °C, some grains grew up to 8 μm in diameter. The relative densities of samples Y1015, Y10125 and Y15175 were found to be lower than 98% at sintering temperatures above 1850 °C. However, samples Y1515 and Y2015 were sintered to a density in excess of 98%, as shown in Fig. 4. With both compositions (Y1515 and Y2015) a maximum in density was achieved at temperatures ranging form 1800 to 1820 °C. Further increase in sintering temperature above ∼1820 °C leads to a gradual decrease in density from ∼99.8% TD down to ∼98.1% at 1920 °C. The reason for the decrease in density above ∼1820 °C is considered to be the decomposition of $Si_3N_4$ into silicon crystal and nitrogen.

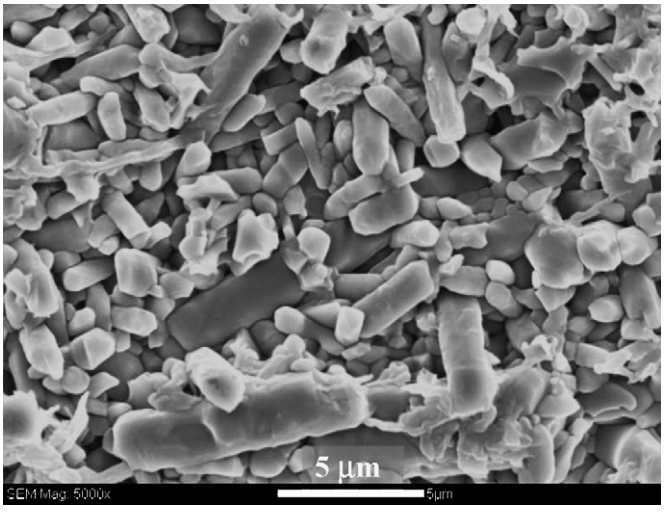


Fig. 2. SEM micrograph of Y1515 sintered at 1800 °C.

In order to evaluate the effect of density on hardness, Fig. 5 displays the variation of hardness with density for Y1515 and Y2015 compositions. As expected hardness of Y1515 increases with increasing relative density and the highest value for hardness (18.2 GPa) is achieved in samples with the highest relative density, i.e., 99.8%. Similar results for the variation of hardness with density were observed in Y2015 samples.

It is interesting to note that the growth of elongated α-SiAlON grains occurred in all single-phase α-SiAlON compositions investigated, suggesting that the self-reinforcement in these compositions is operational and may lead to an enhancement in toughness. In addition to composition, it was found that the sintering temperature has equally important role in promoting the growth of elongated grains and in increasing their volume fraction. In this context, a number of sintering runs were carried out at a wide range of temperatures. Fig. 6 shows the change of the average grain aspect ratio and elongated grain volume fraction for Y2015 samples sintered at temperatures ranging from 1750 to 1850 °C. As the sintering temperature is increased both the average aspect ratio and volume fraction of the elongated grains increase at all temperatures of up to 1850 °C. Above ∼1850 °C, both the grain aspect ratio and the volume fraction of the elongated grains decrease.

The effect of grain aspect ratio and elongated grain volume fraction on fracture toughness for samples sintered at different temperatures is shown in Figs. 7 and 8. The results in Figs. 7 and 8 show clearly that there is linear relationship between fracture toughness and both the grain aspect ration and volume fraction of elongated grains. Unlike aspect ratio and volume fraction of the elongated grain, no defined relationship exists between fracture toughness and grain diameter (grain width). Fig. 9 shows the measured change of fracture toughness as a function of average grain diameter (grain width). Fig. 9 also shows that the maximum value for the grain diameter, which occurs at 1900 °C, does not coincide with the highest value for fracture toughness, which occurs at 1850 °C for Y2015 samples, suggesting that the grain diameter is not a key factor controlling the fracture toughness of Y-α-SiAlONs.

## 4. Discussion

As discussed earlier, the *in situ* formed elongated grains in a single-phase α-SiAlON provide the microstructure with potentials for toughening. In principle there are two possible toughening mechanisms which could operate in Y-α-SiAlON ceramics. One is the crack deflection cause by the crack being forced to change the direction of its propagation from an angle perpendicular to the applied stress to an angle of <90°. The other mechanism which can operate in this system is known as crack bridging. Crack deflection occurs in systems possessing weak interfaces where the propagating crack changes its direction from planar motion (perpendicular to the applied stress) to directions with angles <90° relative to the direction of applied

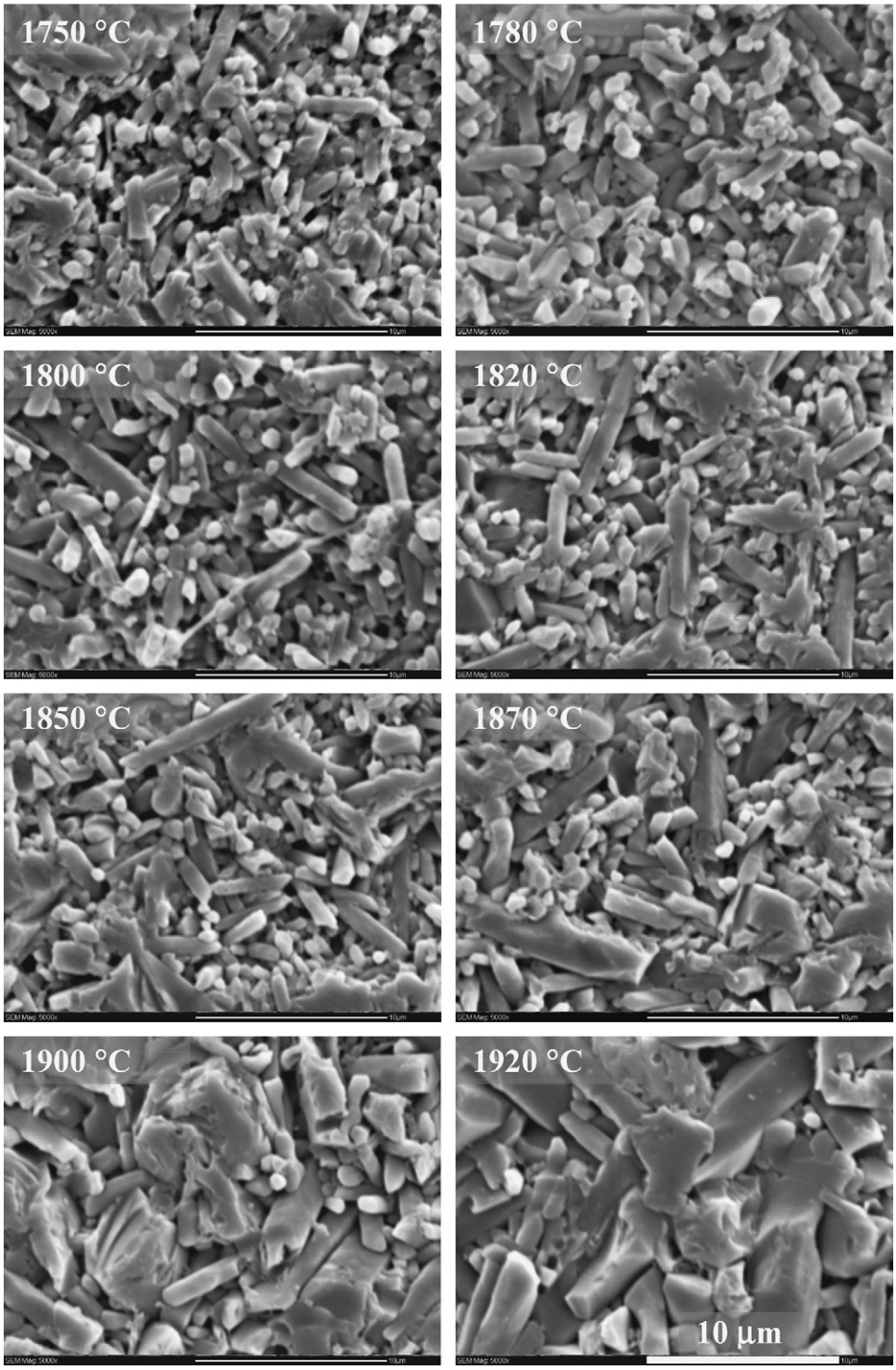


Fig. 3. SEM micrographs of Y2015 sintered at different temperatures.

stress. This change in direction is accompanied by a reduction in stress intensity at the tip of the crack slowing down the crack propagation and increasing the material's resistance to fracture. The bridging mechanism operates most effectively in systems with elongated grains of a high aspect ratio. The contribution of equiaxed grains to toughening in SiAlONs is expected to be minimal.

Assuming that both crack deflection and crack bridging are the two most important mechanisms of toughening in the present system, it would be of interest to determine quantitatively the contribution of each mechanism to the overall toughness of the system. Moreover, it would be important to find out which toughening mechanism dominates the fracture in Y-α-SiAlON ceramics. To quantitatively evaluate the contribution

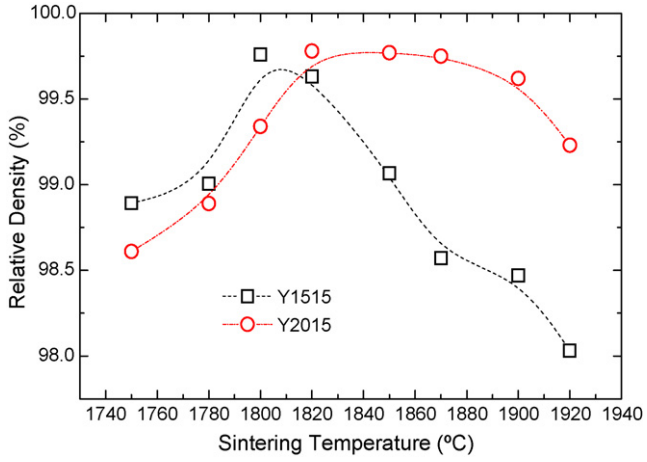


Fig. 4. Relative densities of Y1515 and Y2015 as a function of sintering temperature.

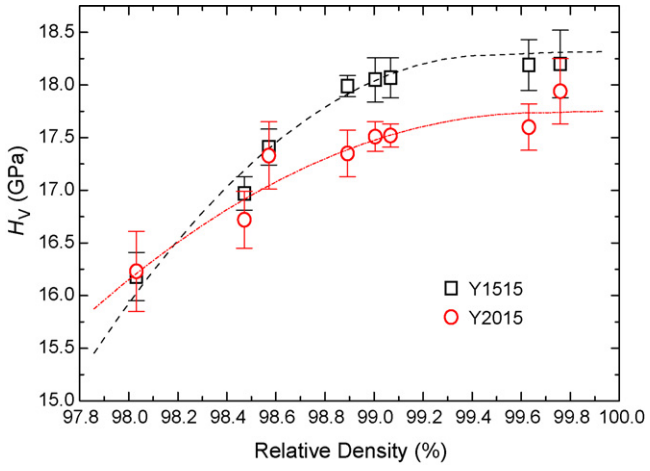


Fig. 5. Change of hardness as a function of relative density for Y1515 and Y2015.

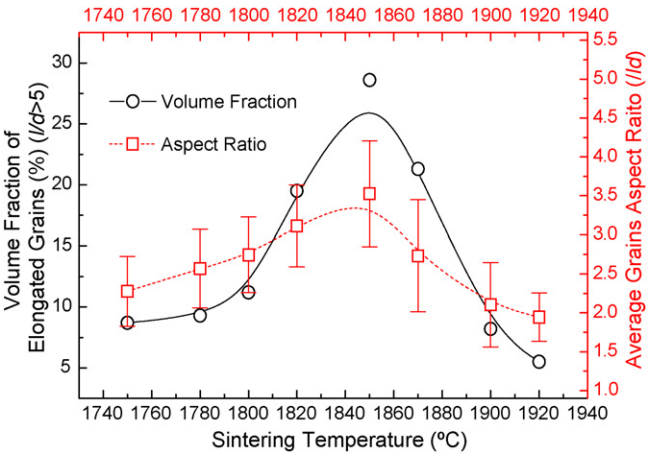


Fig. 6. Volume fraction of elongated grains and average grains aspect ratio of Y2015 as a function of sintering temperature.

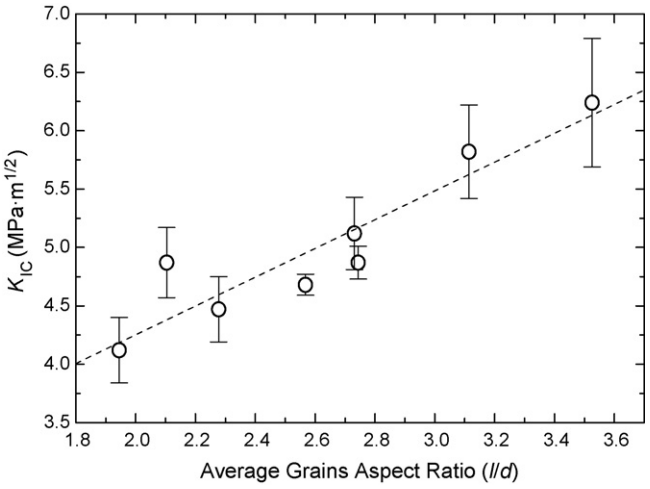


Fig. 7. Fracture toughness of Y2015 as a function of average grains aspect ratio.

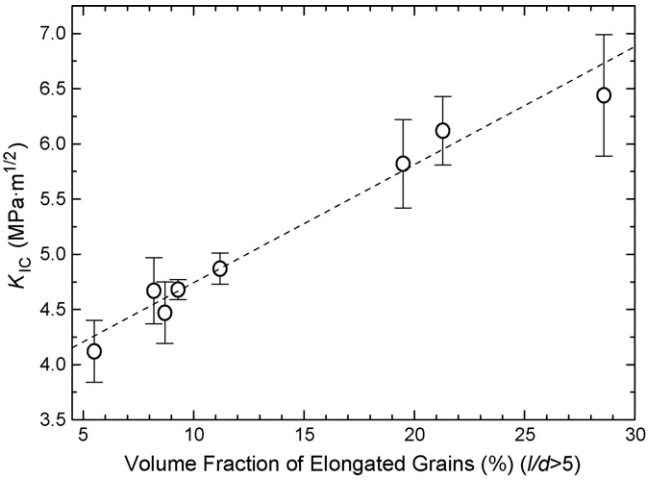


Fig. 8. Fracture toughness of Y2015 as a function of volume fraction of elongated grains.

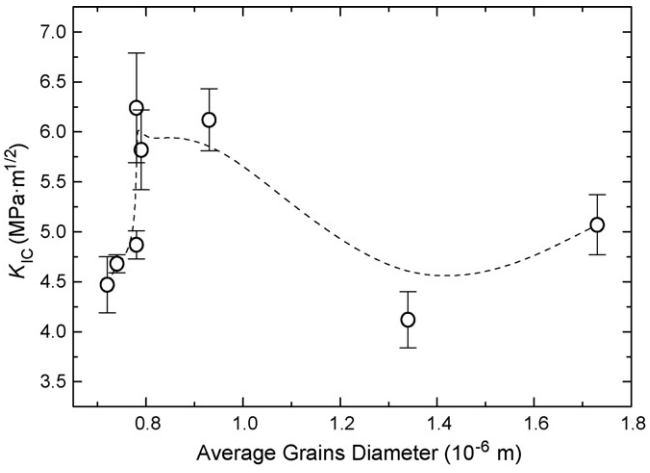


Fig. 9. Fracture toughness of Y2015 as a function of average grains diameter.

from the crack deflection, the expression for fracture toughness developed by Faber and Evans[11] for rod-shaped grains will be employed:

$$K_{IC} = \left\{1 + V\left[0.6 + 0.014\left(\frac{l}{d}\right) - 0.0004\left(\frac{l}{d}\right)^2\right]\right\} K_m \quad (3)$$

where $l/d$ is the average aspect ratio, $V$ the volume fraction of the elongated grains and $K_m$ is the matrix fracture toughness. In order to estimate the contribution of crack deflection to overall toughening, it is necessary first to determine the value for fracture toughness of the ceramics with equiaxed grain structure. This can be done by substituting appropriate values for Young's modulus ($E$), the fracture surface energy ($\gamma_{eff}$) and Poisson's ratio ($\nu$) in the following equation[12]:

$$K_m = \sqrt{\frac{2E\gamma_{eff}}{1-\nu^2}} \quad (4)$$

Based on the values reported for $\gamma_{eff} = 9\,J/m^2$,[13] $\nu = 0.22$ and $E = 320\,GPa$,[14] the fracture toughness of the SiAlON with equiaxed grain is found to be $\sim 2.6\,MPa\,m^{1/2}$. Based on this estimated value for $K_m$ and measured values for the average aspect ratio ($l/d$) of the elongated grains along with their volume fraction, the fracture toughness was calculated using Eq. (3) and presented in Figs. 10 and 11. It is evident that the calculated $K_{IC}$ values (square in Figs. 10 and 11) are only ~50% of experimentally measured values (circle) suggesting that the other mechanism of fracture (crack bridging) also operates in the present system. The contribution of crack bridging mechanism can be estimated using the following equation[15]:

$$K_{IC} = K_m(1 - V) + \left\{\frac{4E\tau Vu}{(1-\nu^2)K_m}\right\}\frac{l}{d} \quad (5)$$

where $K_{IC}$ is the fracture toughness of the system, $K_m$ the fracture toughness of the equaxed grain SiAlON matrix, $V$ the volume fraction of the elongated grains, $u$ the grain pull-out length, $\tau$ the sliding friction stress, $E$ the Young's modulus, $\nu$ the Poisson's ratio and $l/d$ is the grains aspect ratio. According to Eq. (5) the ability of the elongated grains to pull-out during interaction with the crack front depends on the strength of the interface which, in turn, depends on the chemical composition of the boundary phase. As Eq. (5) shows high de-bonding strength ($\tau$) is desirable for high toughness. However, if the de-bonding strength is too high, the pull-out length becomes small thus reducing the crack bridging length and the number of grains bridging the crack. From previous work, it was estimated that only one third of the elongated grains will participate in the crack bridging.[13] The predicted value for fracture toughness due to crack bridging can be obtained by substituting the known values for Young's modulus of 320 GPa,[14] Poisson's ratio of 0.22, the interfacial strength of 100 MPa and the pull-out length of 0.5 μm into Eq. (5).[15] The measured and calculated $K_{IC}$ values (triangle) for Y2015 as function of average aspect ratio and the volume fraction of the elongated grains are presented in Figs. 10 and 11, respectively. Careful analysis of the results in Figs. 10 and 11 reveals that the contribution of crack bridging to the overall fracture toughness is higher than that of crack deflection and proves to be the dominant mechanism of toughening for all compositions studied in this work.

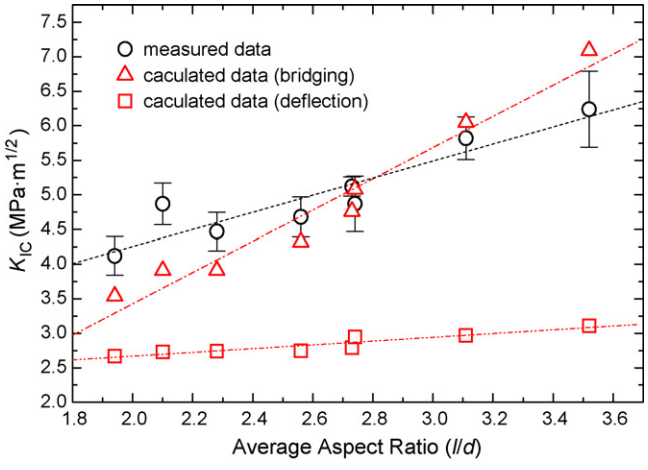


Fig. 10. Measured and calculated values for fracture toughness of Y2015 as function of average grains aspect ratio.

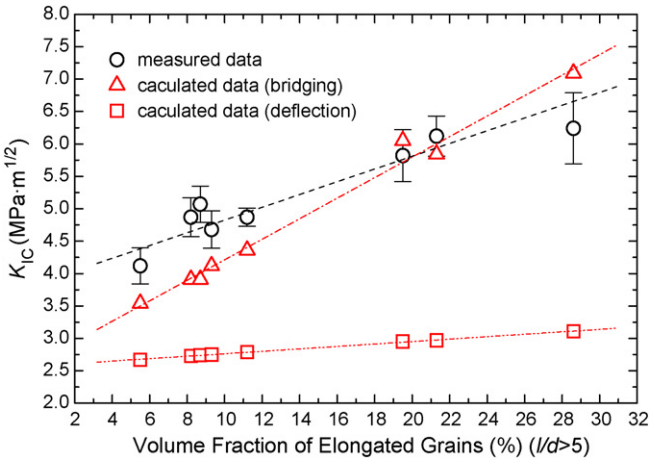


Fig. 11. Measured and calculated values for fracture toughness of Y2015 as function of volume fraction of elongated grains.

## 5. Conclusions

Y-α-SiAlON ceramics can be pressureless sintered to densities in excess of 98% theoretical density at temperatures ranging from 1750 to 1850 °C. Typical microstructure shows elongated α-SiAlON grains uniformly distributed in a matrix of equiaxed grains. The highest fracture toughness of 6.2 MPa m$^{1/2}$ and hardness of 17.6 GPa was found in a single-phase α-SiAlON, designated as Y2015 sintered at 1850 °C. The fracture toughness is affected by both the average aspect ratio and the volume fraction of the elongated grains. No clear relationship was found between fracture toughness and grain diameter/width. The contribution of crack bridging to the overall fracture toughness is higher than that of crack deflection and proves to be the dominant toughening mechanism.

## References


1. Thompson, D. P., In *Tailoring of Mechanical Properties of $Si_3N_4$ Ceramics*, ed. M. J. Hoffmann and G. Petzow. Kluwer Academic Publishers, The Netherlands, 1994, p. 125.
2. Mandal, H., Thompson, D. P. and Ekström, T., Reversible $\alpha \leftrightarrow \beta$ sialon transformation in heat-treated sialon ceramics. *J. Eur. Ceram. Soc.*, 1993, **12**, 421–429.
3. Chen, I.-W. and Rosenflanz, A., A tough SiAlON ceramic based on $\alpha$-$Si_3N_4$ with a whisker-like microstructure. *Nature*, 1997, **389**, 701–704.
4. Wood, C. A., Zhao, H. and Cheng, Y. B., Microstructural development of calcium alpha-SiAlON ceramics with elongated grains. *J. Am. Ceram. Soc.*, 1999, **82**, 421–428.
5. Yu, Z. B., Thompson, D. P. and Bhatti, A. R., Self-reinforment of Li-$\alpha$-sialon ceramics. *J. Mater. Sci.*, 2001, **36**, 3343–3353.
6. Liu, G. H., Chen, K. X., Zhou, H. P., Ning, X. S. and Ferreira, J. M. F., Study of phase transformation and microstructure development of Yb $\alpha$-SiAlON ceramics prepared by pressureless sintering. *Mater. Sci. Forum*, 2005, **475–479**, 1271–1274.
7. Evans, A. G., Ruhle, M., Dalgleish, B. J. and Thouless, M. D., In *Advanced Structural Ceramics*, ed. P. F. Becher, M. V. Swain and S. Sōmiya. Materials Research Society, Pittsburgh, PA, USA, 1987, p. 259.
8. Becher, P. F., Sun, E. Y., Hsueh, C.-H., Alexander, K. B., Hwang, S.-L., Waters, S. B. *et al.*, Debonding of interfaces between beta-silicon nitride whiskers and Si–Al–Y oxynitride glasses. *Acta Mater.*, 1996, **44**, 3881–3893.
9. Evans, A. G. and Charles, E. A., Fracture toughness determinations by indentation. *J. Am. Ceram. Soc.*, 1976, **59**, 371–372.
10. Bjrklund, H., Wasén, J. and Falk, L. K. L., Quantitative microscopy of $\beta$-$Si_3N_4$ ceramics. *J. Am. Ceram. Soc.*, 1997, **80**, 3061–3069.
11. Faber, K. T. and Evans, A. G., Crack deflection processes. I. *Theory Acta Metall.*, 1983, **31**, 565–576.
12. Barsoum, M., *Fundamentals of Ceramics*. McGrow-Hill Companies, USA, 1997.
13. Sun, E. Y., Becher, P. E., Pluchett, K. P., Hsueh, C. H., Alexander, K. B. and Waters, S. B., Microstructural design of silicon nitride with improved fracture toughness. II. Effects of yttria and alumina additives. *J. Am. Ceram. Soc.*, 1998, **81**, 2831–2840.
14. Tanaka, I., Nasu, S., Adachi, A., Miamoto, Y. and Nihara, K., Electronic structure behind the mechanical properties of $\beta$-sialons. *Acta Metall.*, 1992, **40**, 1995–2001.
15. Krstic, V. D., Development of high toughness ceramics by microstructural control. In *Proceedings of International Conference on Engineering and Technological Science 2000-ISAM, Vol 1*, ed. J. Song and R. Yin. Chinese Academy of Engineering, Beijing, China, 2000, p. 83.